IJARIIT INTERNATIONAL JOURNAL OF ADVANCE RESEARCH, IDEAS AND INNOVATIONS IN TECHNOLOGY

ISSN: 2454-132X

Impact Factor: 6.078

(Volume 8, Issue 1 - V8I1-1466)

Available online at: https://www.ijariit.com

Density Functional Theory (DFT) simulations on fullerene/polymer blends for organic photovoltaic systems

Rina Muhammad Faisal
mfaisalrina@gmail.com
University of Colombo, Colombo, Sri Lanka

Professor Rohini de Silva
rohini@chem.cmb.ac.lk
University of Colombo, Colombo, Sri Lanka

Professor K. M. Nalin de Silva
kmnd@chem.cmb.ac.lk
University of Colombo, Colombo, Sri Lanka

ABSTRACT

This research uses computational simulations using SIESTA (Spanish Initiative for Electronic Simulations with Thousands of Atoms) package based on Density Functional Theory (DFT) to explore the free energies, interaction energies, relative stability, stability of bonds and charge transfer abilities of Organic Photovoltaic (OPV) systems comprising of bis[methano- fullerene (6,6)-phenyl-C61-butyric acid methyl ester] (bisPCBM) as the acceptor and eight different donor polymers. The novel donor polymers are computationally designed based on poly[4,8-bis-substituted-benzo [1,2-b:4,5-b']dithiophene-2,6-diyl-alt-4-substituted-thieno[3, 4-b]thiophene-2,6-diyl] (PBDTTT) polymer, the main structural changes being the incorporation of Se and F atoms. From the results it was clear that PCBM makes a wiser choice as the donor compared to bisPCBM for computer simulations. Influence of F atoms was observed in the stability of the system both energetically and structurally. Incorporation of Se negatively affects the feasibility of acceptor-donor interaction.

Keywords: *Density Functional Theory (DFT), Organic Photovoltaic (OPV), Fullerenes, Thiophens, SIESTA*

1. INTRODUCTION

Increasing the power conversion efficiency in organic photovoltaic cells is one of the most sought-after fields in order to find a solution for energy crisis. In an era where current energy demand surpasses the energy supply by various sources, the most prominent being the fossil fuels, the world calls for alternative sources to meet the predicament. This is when scientists diverted their attention to solar power as the amount of sunlight falling on the earth's surface in an hour can fulfil the global energy need of an entire year[1,2]. In the manufacturing process of solar cells, following the breakthrough in inorganic semiconductors, now the attention is primarily on organic semiconductors due to low cost[3], convenient fabrication processes[4], high portability[5], low operating and maintenance costs[5] and compatibility with a wide range of substrates[6]. The electrically conducting organic materials used in Organic Photovoltaic (OPV) devices consist of a donor-acceptor pair through which charge transfer occurs. The electron donor has a low ionization potential and the electron acceptor has a high electron affinity. It is this donor-acceptor pair which plays the key role not only in the organic and super conductors but also in semiconductors[7]. Current OPV devices comprise of organic/inorganic nanostructures like dye- sensitized solar cells[8], multilayers of small organic molecules[9], tandem cells[10] and bulk-hetero junction (BHJ) solar cells[11,12]. The main challenge is to achieve both large photocurrent ***and*** large voltage at the same time. To obtain a large photocurrent, it is necessary to choose materials with a small band gap. This yields a small voltage. If large band gap materials are chosen to achieve a large voltage, a smaller photo current is observed due to the absorption of fewer photons by such materials. Therefore, the major goal in any OPV research is to increase the Power Conversion Efficiency (PCE). It is recommended that in order to improve the PCE of organic photovoltaics, one should improve the Short Circuit Current Density

(Jsc)[13], the Open Circuit Voltage (V_{oc})[14] and the Fill Factor (FF)[13]. Further it has been noticed that the efficiency of exciton formation and dissociation[7,15] as well as the charge transfer between donor and acceptor[7] also affects PCE. It is also necessary to have a broader solar spectrum[13,16-19] and desired morphology[20] to improve PCE.

The V_{oc} of the solar cell is defined as the voltage which recompenses the current flow through the external circuit[9]. The offset between the HOMO (Highest Occupied Molecular Orbital) of the donor and the LUMO (Lowest Unoccupied Molecular Orbital) of the acceptor is often defined as the V_{oc} by most authors[7,9,12,21-24]. Even though many researches are underway to improve the PCE of OPV devices, those which are commercially viable still possess the maximum value within the 10-15% range[25]. Among the highest certified efficiency in the OPV field was recorded for tandem cells by Dou & coworkers[13] which records a PCE of 8.62%, a Jsc of 8.26 mA cm-2, a V_{oc} of 1.56 V and an FF of 66.8%. External Quantum Efficiency (EQE) value of 68.7% at 630 nm achieved by Chen et al.[26] with low band gap polymer solar cells was also among the highest reported so far. Their certified efficiency was 6.77% while the average obtained efficiency was 7.38%. Our research is mainly influenced by two investigations; one is the study carried out by Chen et al.[26], who has shown that both the HOMO and the LUMO level of donor poly[4,8-bis-substituted-benzo[1,2-b:4,5-b']dithiophene-2,6-diyl-alt-4-substituted-thieno[3, 4b]thiophene-2,6-diyl] (PBDTTT-E) can be lowered by introducing two modifications. One is to replace the alkyloxy group on the carbonyl of the thieno[3,4-b]thiophene unit with an alkyl side chain (this molecule is referred to as PBDTTT-C) without changing the band gap. The second is the introduction of Fluorine atom (this molecule is referred to as PBDTTT-CF). The second is the study by Liang et al.[14] where introduction of fluorine, an atom of high electron affinity, to the thieno[3,4-b]thiophene unit has shown to increase the Voc and hence demonstrating a PCE of 6.1%. According to their study, the application of a functional group leads to simultaneous change for both HOMO and LUMO levels. In most of the other systems a change occurs only in either of the levels, not in both. Considering the above influences, the primary goal of our research was to investigate Bulk Hetero Junction (BHJ) solar cells through the design of novel organic donors using computational simulations based on Density Functional Theory (DFT). Our research used computational simulations to investigate the free energies, interaction energies, relative stability, stability of bonds and charge transfer abilities of OPV systems comprising of bis[methano- fullerene (6,6)-phenyl-C61-butyric acid methyl ester] (bisPCBM) as the acceptor and eight different donor molecules based on novel, computational modifications to PBDTTT-C molecules which includes incorporation of F atoms and replacement of S atoms with Se in order to study their effectiveness in OPV systems.

2. MATERIALS AND METHODS

Design and simulations of molecules of interest were conducted using HP Compaq Pro 6300 Desktop Computers with Intel i5 350M 3rd Generation processors, 4 GB RAM and 500 GB Hard Disks. Windows 8.0 and Ubuntu 14.04 comprised the operating systems of these computers. Designing of molecules and OPV systems were performed using Gauss View 5.0. Simulations on these molecules were done using Gaussian 98 and SIESTA-3.2 programs. To view the output structure XCrySDen program was used. Data analysis by plotting the required graphs was done using Grace plotting tool. Out of these software packages, SIESTA, XCrySDen and Grace Programs run on the Ubuntu 14.04 OS while Gauss View 3.0 and Gaussian 98W were run on Windows 8.1 OS. Parallel compilation was used for simulations in SIESTA using the 'mpif90' compiler. MPICH2, BLAS, Lapack-3.2 and Scalapack-3.2 were the additional library packages which were used. In the 'FDF' file (Flexible Data Format) of SIESTA simulations, 'PAO.BasisSize' and 'AO.BasisType' were defined to be 'Split' and 'Standard' (with DZP for each Chemical Species) respectively. Generalized Gradient Approximation (GGA) was chosen to be the 'XC.functional' parameter while Conjugate Gradient (CG) was chosen to be the 'MD.TypeofRun' parameter. The pseudo potential files which contain the mathematical approximation for the electrons of the inner orbitals were downloaded from the standard library of the SIESTA. The 'rho2xsf' utility facility which facilitates the viewing of many replicas of the periodic boundary cell was used. Mulliken Population Analysis was carried out to study charge transfer occurrences. Initially, individual simulations were conducted on the bisPCBM molecule (acceptor) (Figure 1 (a)) and PBDTTT-C monomer unit (considered as the 'benchmark donor' molecule) (Figure 1(b)).

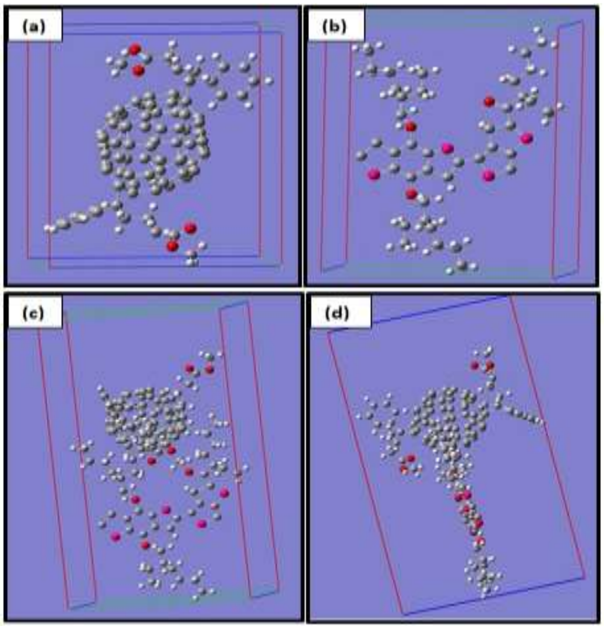

Figure 1: (a)bisPCBM-the acceptor; (b)PBDTTT-C-the benchmark donor; (c)&(d)The benchmark OPV system front and side view respectively.

Then followed the simulations on the 'benchmark OPV system' which comprises of the above mentioned bisPCBM acceptor molecule and PBDTTT-C donor monomer unit (Figure 1(c) & (d)). Then individual simulations were carried out on the eight newly designed donor polymers which are demonstrated in Figure 7 and attached to the end of the article. This was followed by individual simulations on each 'bisPCBM acceptor – new modified PBDTTT-C donor' pair with 1:1 ratio in order to control the computational cost. The results were analysed with respect to the 'benchmark donor' molecule and the 'benchmark OPV system'. Note that the diagrams, Figure 2 - Figure 9 (except Figure 7) are those viewed from XCrySDen software where the C atoms are in yellow, H in blue, O in red, S in magenta, Se in green and F in violet.

It is important to note that this software does not recognize a bond beyond a certain bond length and hence the bond is not displayed. Mostly the double bond would be displayed as single bond since it's just a graphical representation. Therefore, to get precise analysis on bond lengths of the structure, the actual distance was to be calculated. Discussion on bond lengths were based on standard bond lengths of organic compounds derived from X-ray Crystallographic Studies[27] which can be found annexed to Appendix 1 of Supplementary Materials.

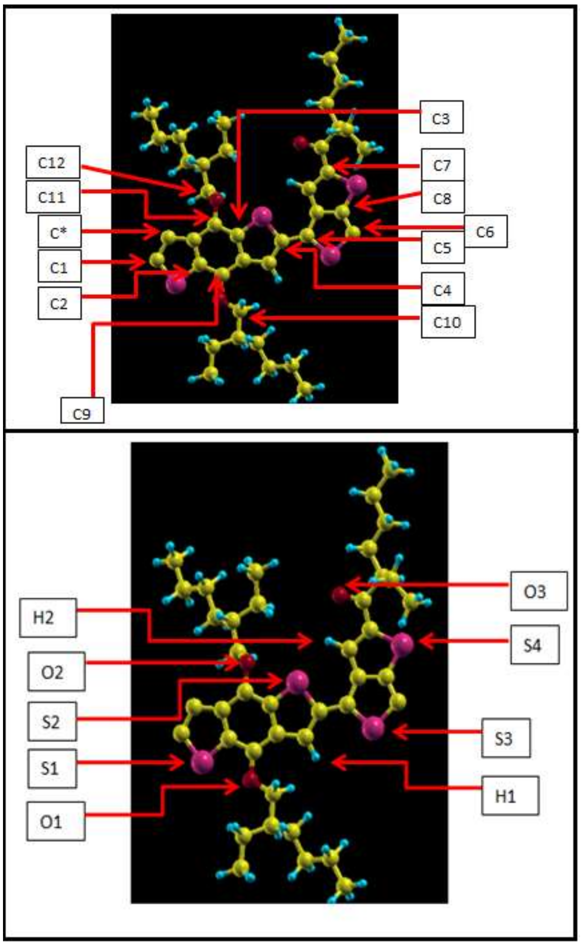

Figure 2: Customized labeling of atoms

Figure 2 shows the customized labeling of atoms in the donor polymer which had been used in sections ahead. When S was replaced by Se, they had been numbered similarly as Se1, Se2, Se3 and Se4. Likewise, when H is replaced by F, they had been named as F1 and F2.

3. RESULTS AND DISCUSSION

This research had yielded quantitative results for analysis of bond lengths, free energies, interaction energies, relative stabilities and charge transfer of the systems simulated.

Analysis of bond lengths in benchmark OPV systems

When considering the optimized bisPCBM structure (Figure 3(a)), one of the ester components had remained intact while the second had been fragmented from the whole structure. Analysis of bond lengths of the attached ester component shows that, the C-C connecting the fullerene are 2.9021 Å (this was considered as bond 1) and 3.0992 Å (this was considered as bond 2) in length. The possible reasons for fragmentation of the ester moiety can be attributed to lower stability of bisPCBM compared to PCBM or interaction with the donor polymer from the neighbouring cells. Observations of the original donor- PBDTTT (Figure 3(b)) shows that the structure remained intact and the bond lengths correspond to the standard bond lengths of the original species. Observation of the front view of benchmark OPV system (Figure 4) shows a detached H confirming the charge transfer taking place[28]. Also, the C12-O2 bond had been detached with a distance of 3.3913 Å. As there was a charge transfer between bisPCBM and the donor polmer, a part of the donor polymer could have been broken to narrow the gap (between the donor polymer and bisPCBM) which led to the detachment.

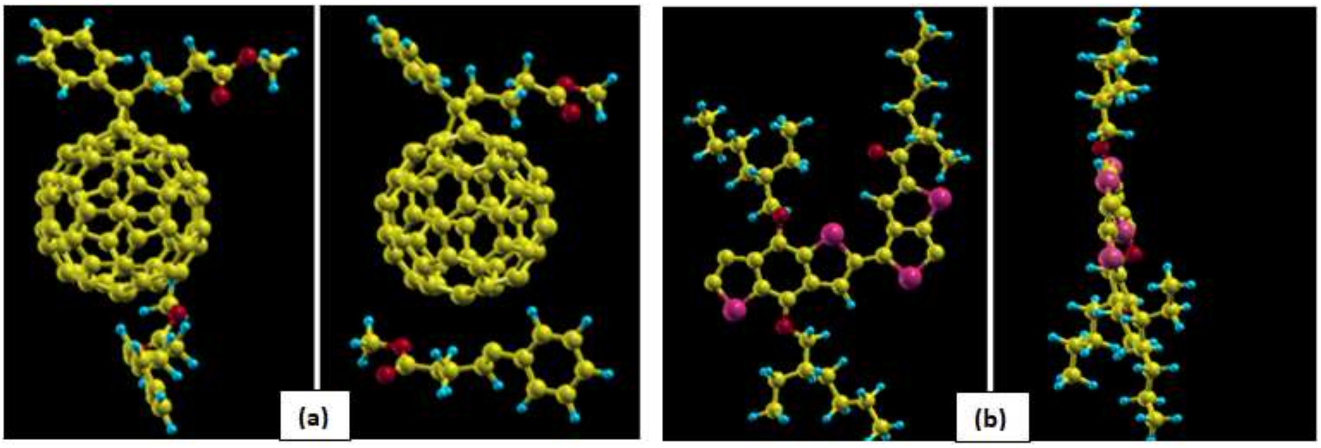

Figure 3: (a) Optimized bisPCBM- Front (L) view and Side (R) view; (b) Optimized PBDTTT-C - Front (L) view and Side view(R)

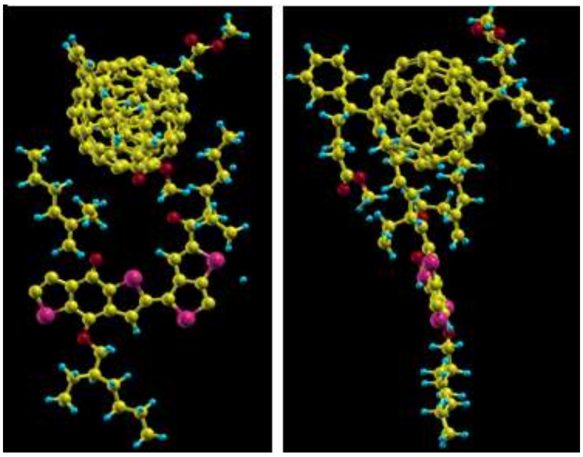

Figure 4: Optimized Benchmark OPV system - Front (L) view and Side (R) view

Interestingly, the side view of the benchmark OPV system (Figure 4) illustrates the detached ester component of bisPCBM which had bonded back to fullerene through a single bond. The bond length is 1.5364 Å which correlates well with reported single C-C bond lengths[27]. This emphasizes the stability of bisPCBM in the presence of the donor than when it is simulated alone. Optimized structures of different donors and OPV systems that had been carried out are demonstrated in Figure 8 and Figure 9 respectively and attached to the end of the article. As seen in the individual simulations of bisPCBM, in all of these systems, one of the ester components remained intact while the other had been fragmented from the whole structure.

Analysis of C-C bond lengths

Table 1 shows the deviation of bond lengths in the OPV systems when 2.9021 Å and 3.0992 Å are taken as reference points for the two carbon bonds connecting the nondetached ester moiety to fullerene while their graphical illustration is given in Figure 5(a).

Table 1: C-C Bond lengths between the fragmented ester component and fullerene in OPV systems (Å)

System	Bond 1	Bond 2	Deviation of Bond 1	Deviation of Bond 2
PV1	2.7754	3.2026	-0.1267	+0.1034
PV2	2.8363	3.1823	-0.0658	+0.0831
PV3	2.7843	3.0785	-0.1178	-0.0207
PV4	2.8418	3.1752	-0.0603	+0.0760
PV5	2.7464	3.1214	-0.1557	+0.0222
PV6	3.0258	3.1784	+0.1237	+0.0792
PV7	2.7754	3.2026	-0.1267	+0.1034
PV8	3.0549	3.2101	+0.1528	+0.1109

Observation of the graph shows that the variation of bond 2 in all the OPV systems from that of the benchmark molecule is still within the acceptable range.

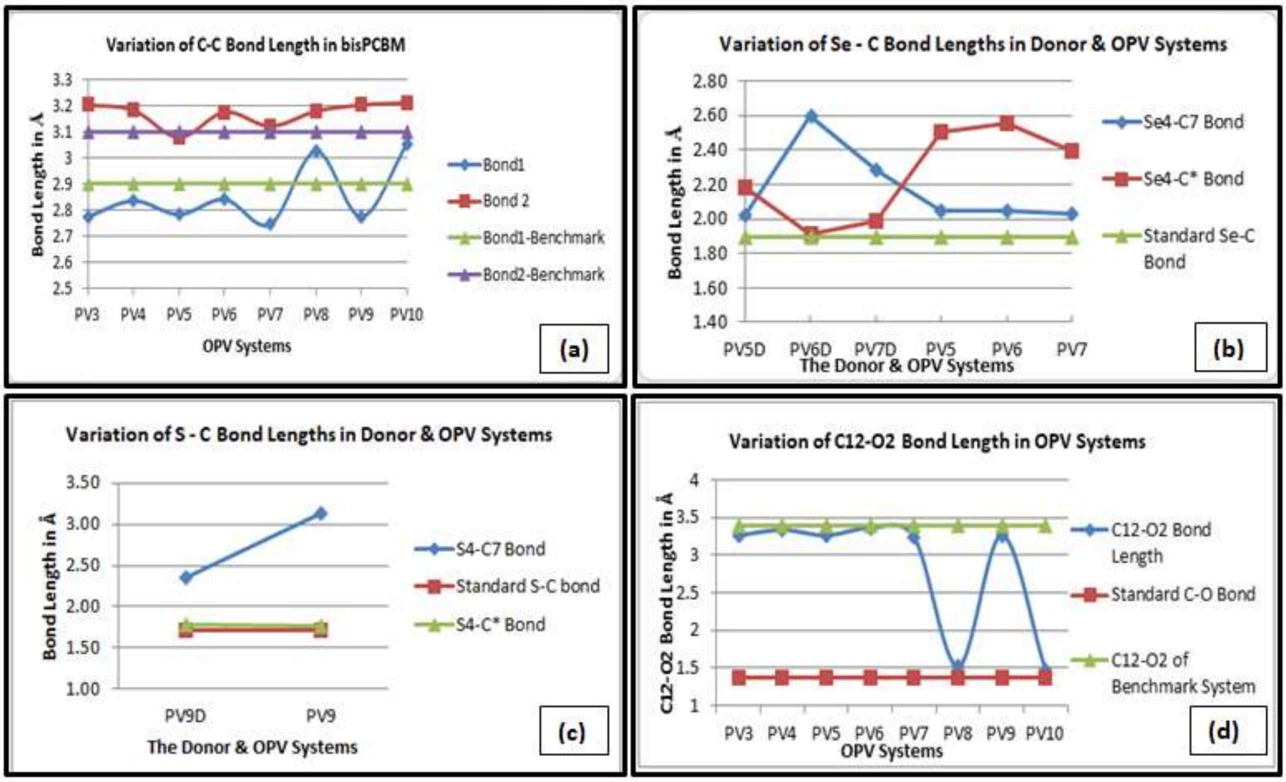

Figure 5: (a) Variation of C-C bond length in bisPCBM of OPV systems; (b) Variation of Se-C bond length in Donor and OPV systems; (c) Variation of S-C bond length in Donor and OPV systems; (d) Variation of C12-O2 bond length in OPV Systems

Similarly, the variation of bond 1, except for PV5, falls within the accepted range. Even though bond 1 of PV6 and PV8 deviates from the bond 1 length of benchmark molecule, the values were comparable with that of bond 2 and are still within the acceptable range for C-C bond lengths. These observations clearly highlighted the structure stability of PCBM compared to that of bisPCBM in computer simulation environments.

Analysis of S-C and Se-C bond lengths in donors

Detachment of certain S-C and Se-C bonds were observed which includes Se4-C7 bonds of the donors PV3D, PV4D, PV5D and S4-C7 bond of the donor PV7D in both the simulated donor systems and their respective OPV systems. This was observed when the output structure in one particular periodic cell was studied. When the periodic images of the donor systems were analyzed, a remarkable change can be seen in the bonding patterns of PV4D, PV5D and PV7D which explains the breaking of the above bond. A new bond has been formed between C* of one monomer unit and the S4 (or Se4) of the adjacent monomer unit thus giving rise to 5 heterocyclic rings consecutively. On the other hand, when the periodic images of the OPV Systems were studied, the 5 consecutive heterocyclic rings were observed only in PV7 and not in PV4 or PV5. Figure 5(b) graphically represents data about Se-C bonds. It can be easily observed that, with regard to the donor systems PV4D and PV5D, the newly formed Se4-C* bond was in the range of standard bond length while the originally present Se4-C7 bond deviated much further from this value; this confirmed the stability of the newly formed structure, compared to the original. However, Se-C* bond lengths in PV4 and PV5 OPV systems deviated from ideal bond lengths while Se4-C7 was comparable with standard bond lengths. This demonstrated that although there's a tendency for the donors to form 5 heterocyclic rings, the presence of the bisPCBM acceptor prevents this possibility. The Donor system PV7D and its OPV system (PV7), shows the most remarkable structural changes of all the systems. The newly formed S4-C* bond is in perfect alignment with the standard S-C bond length as graphically represented in Figure 5(c). The originally present S4-C7 deviates much farther from this value.

Analysis of C-O bond lengths in the donors of OPV systems

Just as in the benchmark OPV system, disintegration of the C12-O2 bond is clearly visible in all the OPV systems except PV6 and PV8. Figure 5(d) graphically represents the variation of C12-O2 bond lengths of the donors in the OPV systems and their deviation from that of the benchmark system and standard C-O bond length. According to the graph, the C12-O2 bonds of the PV6 and PV8 systems were comparable with that of standard C-O bond length while the rest of the systems are in accordance with that of the benchmark OPV systems. Observation of the structures indicated the presence of 2 Se atoms (in the 2nd and 3rd positions) and an F atom in the F1 position as the common features in both PV6 and PV8. However, having an additional F (in F2 position) in PV8 had not influenced any changes on C-O bond length. This effect can be further compared by observing PV7 (which comprises of 2S, 2Se in 2nd & 3rd positions and an F in F2 position) where the C-O bond length was found to be within the same range as PV8. Also, this behavior was not exhibited by PV3 and PV5 systems (which comprised of 1 F atom in F1 position with no S atoms). Hence it can be concluded that the two S atoms at the 1st and 4th positions as well as the F atom in F1 position had influenced the stability of the C12-O2 bond, preserving the intact structure of the designed donor.

Other major structural changes

Detached H atoms seen in all systems showed evidence for the presence of charge transfer. The most significant change can be seen in PV7 where quite unexpectedly, an HF molecule has been formed (between a detached H and F2 atom). The H-F bond is 0.94 Å which is in line with published data [27].

Analysis of Free energies and relative stability

Table 2 given below states the total free energies of the Donor systems, the OPV systems and the benchmark systems (where PVOrg and PVOrgD stand for Original OPV system and Original Donor respectively) in units of eV. Analysis of the tabulated energy values showed that all systems possess a high negative value for free energy.

Table 2: Free Energies and relative stability of donors and OPV systems

System Name	Free Energy (eV)	Relative Stability
OPV Systems		
PV1	-25668.94	0.997
PV2	-25587.21	0.994
PV3	-26237.69	1.019
PV4	-26240.42	1.019
PV5	-26893.83	1.044
PV6	-26319.49	1.022
PV7	-26319.29	1.022
PV8	-26973.18	1.048
Donor Systems		
PV1D	-9831.20	0.992
PV2D	-9753.66	0.984
PV3D	-10407.06	1.050
PV4D	-10406.32	1.050
PV5D	-11059.50	1.116
PV6D	-10484.50	1.058
PV7D	-10483.19	1.058
PV8D	-11137.66	0.992
Benchmark Systems		
bisPCBM	-15834.50	NA
PVorgD	-9908.78	NA
PVOrg	-25748.59	NA

Column 3 shows the relative stability of each system compared to the respective benchmark system (e.g. PV1: PVOrg and PV1D: PVOrgD). The OPV systems PV1 and PV2 are less stable than the benchmark OPV system while PV3 to PV8 are more stable. In Donor systems, PV1D, PV2D and PV8D are less stable than the benchmark Donor system while others show a higher stability. However, the stabilities can be considered to be equal to that of the benchmark systems as the values are very much closer to those of benchmark systems. The graphical representation of above data is shown in Figure 6(a) for Donor Systems and Figure 6(b) for OPV Systems. The shapes of the curves in both the graphs were much similar. Accordingly, PV8 seems to be the most stable followed by PV5. The common feature between PV5 and PV8 is that both of them contain two F atoms (in F1 and F2) positions. The OPV systems, PV6 and PV7 exhibited similar free energies. They both contain 2 S and 2 Se atoms and one F atom. Similar observation can be seen in PV3 and PV4 as well where they possess 4 Se atoms and no S atoms. Similar to PV6 and PV7, they contain one F atom on each. Also the free energies of PV 3, 4, 6 and 7 fall within a similar range as seen from the graph. Compared to all systems PV1 and PV2 seem the least stable and have similar energies. It can be noted that they possess 2S, 2Se atoms and 0S, 4Se atoms respectively. Both the systems do not contain any F atoms. The exact same observations can also be made in their respective donor systems as visualized in Figure 6(a). From these observations, it is clear that the presence and the number of F atoms play a major role in the Free Energies of the system while no such influence was observed with Se atoms.

Analysis of Interaction energies

The interaction energies of the systems were calculated using Equation 1 given below:

$$E_{interaction} = E_{system} - E_{donor} - E_{bisPCBM} \qquad (1)$$

The values in eV and kJ mol^{-1} are tabulated in Table 3. Figure 6(c) represents this data graphically. As it can be observed from the data, the interaction energy is the highest negative for the benchmark OPV system followed by PV1. High negative energy showed by OPV systems, PV1, PV6, PV7 and PV8 confirmed higher interactions between donor and acceptor. In contrast, positive values obtained for OPV systems PV2 to PV5 demonstrated inability of interaction between the acceptor and the donor.

Table 3: Interaction Energies of the Systems

System	Interaction Energy (eV)	Interaction Energy (kJ per mol)
PV1	-3.23	-312.06
PV2	0.96	92.19
PV3	3.87	373.75
PV4	0.40	38.99
PV5	0.16	15.52
PV6	-0.49	-47.09
PV7	-1.60	-154.13
PV8	-1.02	-98.21
PVOrg	-5.30	-511.80

It's worthwhile to note that the OPV systems portraying a negative interaction energy were those with 2 Se atoms and 2 S atoms (PV 1,6,7 and 8) while those with a positive interaction energy are systems with 4 Se atoms (no S atoms).

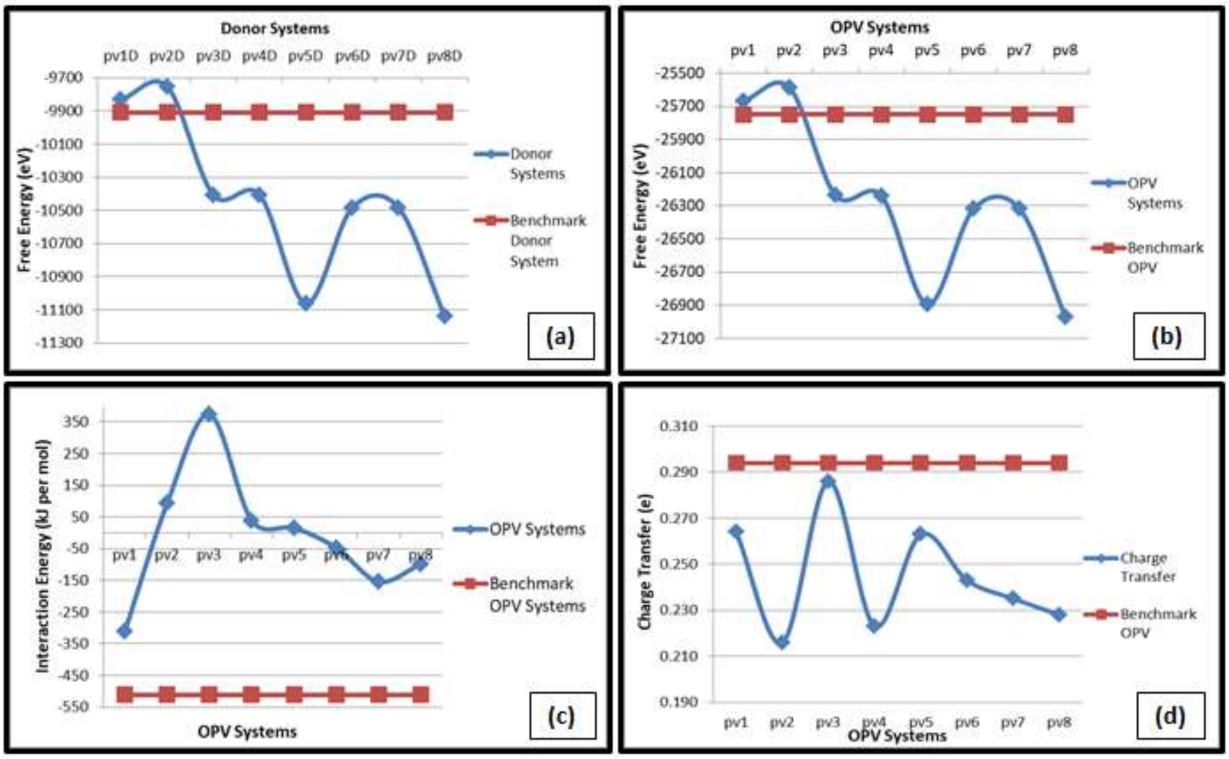

Figure 6: (a) Free Energies of Donor Systems; (b) Free Energies of OPV systems; (c) Interaction Energies of OPV Systems; (d) Charge transfer in OPV systems

Clearly, the number of Se atoms in the system plays a major role in the feasibility of acceptor – donor interaction according to this data. Also, it is clear that the feasibility with 4 Se atoms is lesser than with 2 Se atoms.

Analysis of charge transfer from donor to acceptor

Charge transfer between the donor and the acceptor was calculated by analysing the certain SIESTA utility packages and a simple code written using FORTRAN. The evaluated data is presented in Table 4 below.

Table 4: Charge Transfer in the OPV systems

System Name	Charge Transfer (e)
PV1	0.264
PV2	0.216
PV3	0.286
PV4	0.223
PV5	0.263
PV6	0.243

PV7	0.235
PV8	0.228
Benchmark OPV	0.294

Figure 6(d) shows the graphical representation of Table 4. As it can be seen, significant changes among systems was not observed despite the vast structural and energetic changes the different systems portrayed. Nevertheless, the Benchmark OPV system showed the highest amount of charge transfer while next highest was PV3. The two least ones are PV2 and PV4 both of which comprised of 4 Se atoms and no S atoms. However, this cannot be considered the reason as the third system with 4 Se atoms and no S (i.e. PV3) shows a much higher charge transfer. In order to achieve efficient charge transfer between the donor and acceptor, a donor:acceptor weight ratio of 2:1 or 3:1 is ideal. Since the molar weight of bisPCBM and the benchmark donor are approximately equal to 1100 and 707 g mol^{-1}, a 2:1 and 3:1 weight ratio should yield a molar ratio of 3.11 and 4.66 respectively.

For all PV systems (i.e. PV1 – PV8), 1:1 donor acceptor ratio was used due to higher computational times observed with other high ratios.

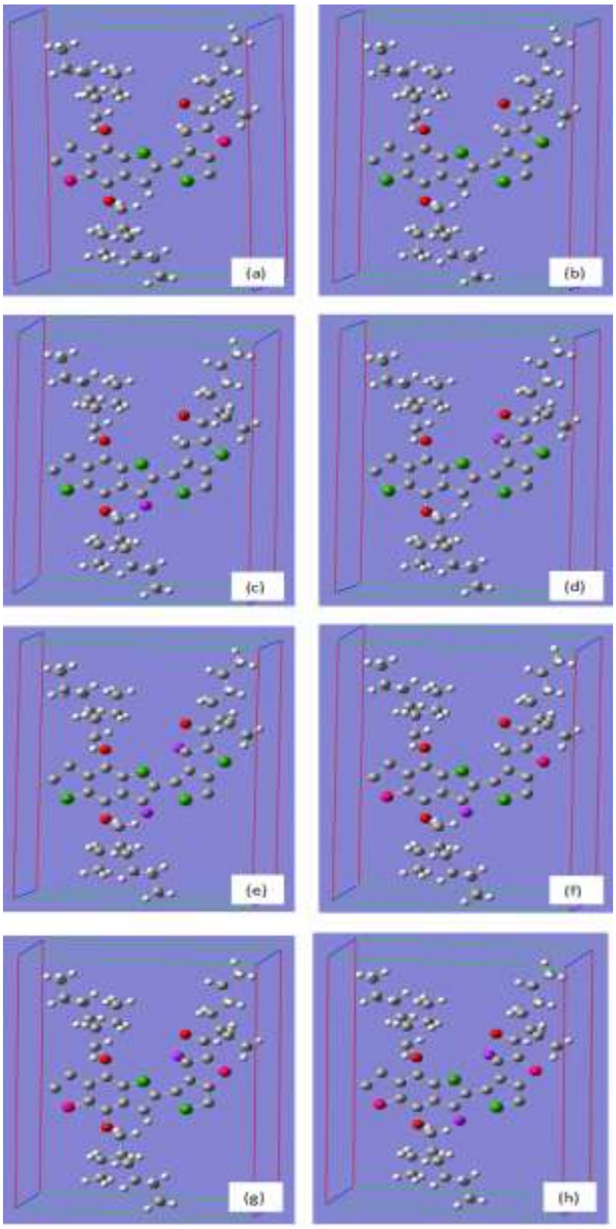

Figure 7: Design of novel donors based on PBDTTT-C designed using Gauss View

(a) PV1D: 2 S atoms, 2 Se atoms (2nd and 3rd positions), No F atoms
(b) PV2D: 0 S atoms, 4 Se atoms, No F atoms
(c) PV3D: 0 S atoms, 4 Se atoms), 1 F atoms (F1 position)
(d) PV4D: 0 S atoms, 4 Se atoms, 1 F atoms (F2 position)
(e) PV5D: 0 S atoms, 4 Se atoms, 2 F atoms (F1 and F2 positions)
(f) PV6D: 2 S atoms, 2 Se atoms (2nd and 3rd positions), 1 F atoms (F1 position)
(g) PV7D: 2 S atoms, 2 Se atoms (2nd and 3rd positions), 1 F atoms (F2 position)
(h) PV8D: 2 S atoms, 2 Se atoms (2nd and 3rd positions), 2 F atoms (F1 and F2 positions)

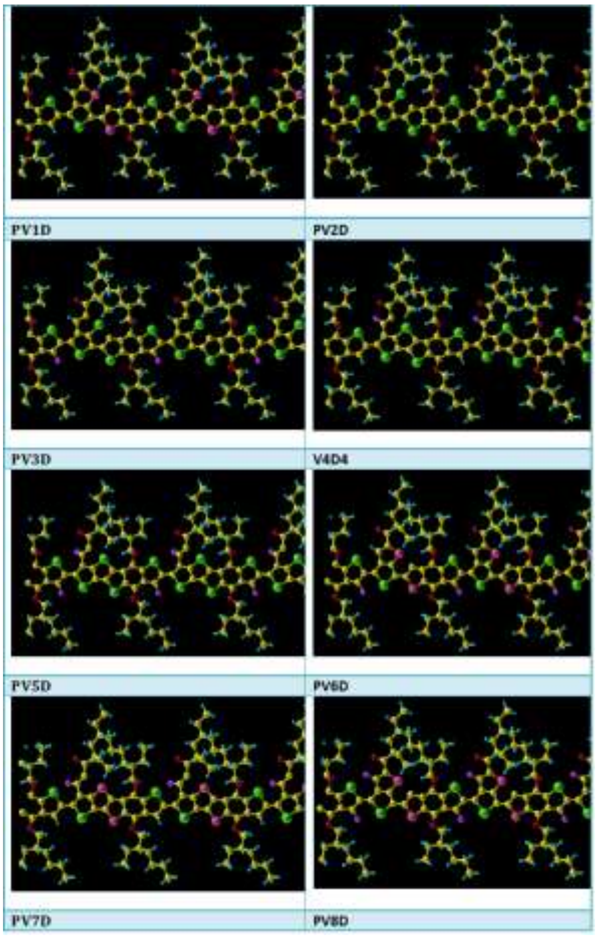
PV1D PV2D
PV3D V4D4
PV5D PV6D
PV7D PV8D

Figure 8: Optimized Structures of Donors

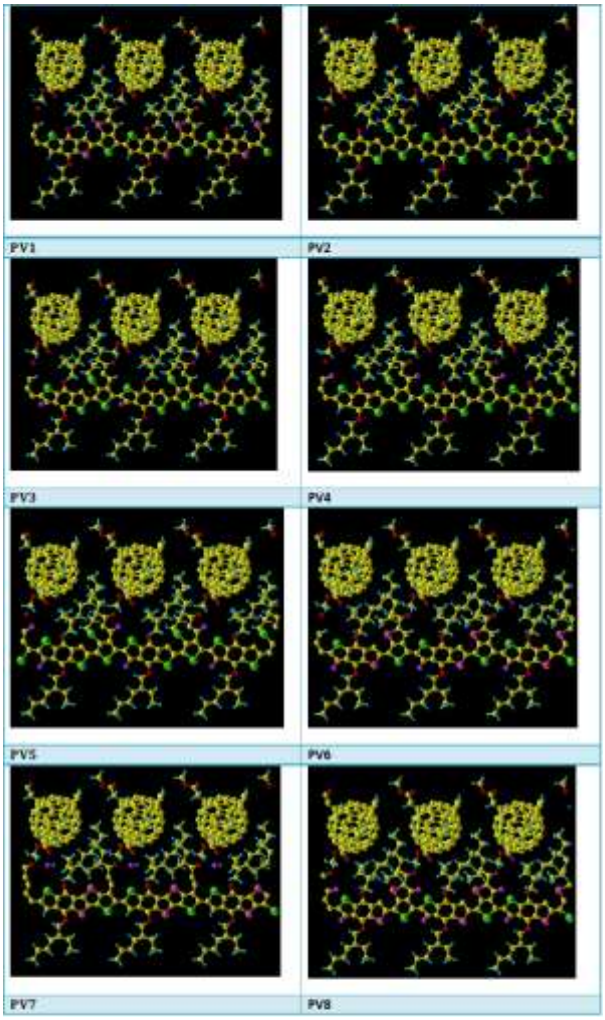
PV1 PV2
PV3 PV4
PV5 PV6
PV7 PV8

Figure 9: Optimized Structures of OPV systems

4. CONCLUSIONS

It can be concluded that bisPCBM makes an efficient acceptor when coupled with the original donor molecule while PCBM is preferable for the other modified donors. Only one modified donor (PV7D) portrayed the successful formation of five consecutive heterocyclic rings for both the donor system and the OPV system. While the donors PV4D and PV5D did establish five consecutive heterocyclic rings in their individual simulation, the presence of bisPCBM has prevented in achieving this goal in their respective OPV systems. This implies that the charge transfer has occurred between the donor and the acceptor in both the systems. Although PV7D seemed to be an ideal candidate showing all appropriate properties, it fails as an OPV system due to occurrence of charge transfer within the molecule (dark current) which confirmed the formation of HF. Also it can be concluded that the two S atoms (1st and 4th positions) and the F atom in F1 position help to preserve the stability of C12-O2 bond and keep the alkyloxy moiety intact with donor polymer. From the analysis of the experimental results, it's evident that the presence of F atoms in the donor backbone plays an important role in the free energies of the systems although no such impact is evident due to Se. Higher the number of F atoms, higher the stability of the conjugated donor. Accordingly, PV5D and PV8D were the most stable among all donor polymers and their respective OPV systems. The results also revealed that the presence of Se plays a negative role in the feasibility of the donor-acceptor interaction.

5. SUPPLEMENTARY MATERIALS

Supplementary Materials consists of two appendices. Appendix 1 tabulates the standard bond lengths of organic compounds according to published data[27]. Appendix 2 contain the corresponding tables for the figures "Figure 5b", "Figure 5c" and "Figure 5d".

6. REFERENCES

[1] Crabtree, G.W. and Lewis, N.S., 2007. Solar energy conversion. Physics today, 60(3), pp.37-42.

[2] Barber, J., 2009. Photosynthetic energy conversion: natural and artificial. Chemical Society Reviews, 38(1), pp.185-196.

[3] Shaheen, S.E., Ginley, D.S. and Jabbour, G.E., 2005. Organic-based photovoltaics: toward low-cost power generation. MRS bulletin, 30(1), pp.10-19.

[4] Günes, S., Neugebauer, H. and Sariciftci, N.S., 2007. Conjugated polymer-based organic solar cells. Chemical reviews, 107(4), pp.1324-1338.

[5] Brabec, C. J., Hauch, J. A., Schilinsky, P., Waldauf, C., 2005. Production aspects of organic photovoltaics and their impact on the commercialization of devices. MRS bulletin, 30(1), pp. 50-52.

[6] Kroon, R., Lenes, M., Hummelen, J.C., Blom, P.W. and De Boer, B., 2008. Small bandgap polymers for organic solar cells (polymer material development in the last 5 years). Polymer Reviews, 48(3), pp.531-582.

[7] Beljonne, D., Cornil, J., Muccioli, L., Zannoni, C., Brédas, J.L. and Castet, F., 2011. Electronic processes at organic− organic interfaces: Insight from modeling and implications for opto-electronic devices. Chemistry of Materials, 23(3), pp.591-609.

[8] Grätzel, M., 2003. Dye sensitized solar cells. Journal of Photochemistry and Photobiology C: Photochemistry Reviews, 4(2), 145-153.

[9] Scharber, M.C., Mühlbacher, D., Koppe, M., Denk, P., Waldauf, C., Heeger, A.J. and Brabec, C.J., 2006. Design rules for donors in bulk-heterojunction solar cells—Towards 10% energy-conversion efficiency. Advanced materials, 18(6), pp.789-794.

[10] Ameri, T., Dennler, G., Lungenschmied, C. and Brabec, C.J., 2009. Organic tandem solar cells: A review. Energy & Environmental Science, 2(4), pp.347-363.

[11] Hoppe, H. and Sariciftci, N.S., 2006. Morphology of polymer/fullerene bulk heterojunction solar cells. Journal of Materials Chemistry, 16(1), pp.45-61.

[12] Dennler, G., Scharber, M.C. and Brabec, C.J., 2009. Polymer-fullerene bulk-heterojunction solar cells. Advanced materials, 21(13), pp.1323-1338.

[13] Dou, L., You, J., Yang, J., Chen, C.-C.,He, Y., Murase, S., Moriarty, T., Emery, K., Li, G., Yang, Y., 2012. Tandem Polymer Solar Cells Featuring a Spectrally Matched Low-bandgap Polymer. Nature Photonics, 6, pp.180-185.

[14] Liang, Y., Feng, D., Wu, Y., Tsai, S.T., Li, G., Ray, C. and Yu, L., 2009. Highly efficient solar cell polymers developed via fine-tuning of structural and electronic properties. Journal of the American Chemical Society, 131(22), pp.7792-7799.

[15] Brédas, J.L., Norton, J.E. and Corniel, J., 2009. Molecular understanding of organic solar cell: the challenges. Accounts of Chemical Research, 42(11), pp.1691-1699.

[16] Chou, C.H., Kwan, W.L., Hong, Z., Chen, L.M. and Yang, Y., 2011. A metal-oxide interconnection layer for polymer tandem solar cells with an inverted architecture. Advanced Materials, 23(10), pp.1282-1286.

[17] Kim, J.Y., Lee, K., Coates, N.E., Moses, D., Nguyen, T.Q., Dante, M. and Heeger, A.J., 2007. Efficient tandem polymer solar cells fabricated by all-solution processing. Science, 317(5835), pp.222-225.

[18] Gilot, J., Wienk, M.M. and Janssen, R.A., 2010. Optimizing polymer tandem solar cells. Advanced Materials, 22(8), pp.E67-E71.

[19] Sista, S., Park, M.H., Hong, Z., Wu, Y., Hou, J., Kwan, W.L., Li, G. and Yang, Y., 2010. Highly efficient tandem polymer photovoltaic cells. Advanced materials, 22(3), pp.380-383..

[20] Sumpter, B.G. and Meunier, V., 2012. Can computational approaches aid in untangling the inherent complexity of practical organic photovoltaic systems?. Journal of Polymer Science Part B: Polymer Physics, 50(15), pp.1071-1089.

[21] Huo, L., Hou, J., Zhang, S., Chen, H.Y. and Yang, Y., 2010. A Polybenzo [1, 2-b: 4, 5-b′] dithiophene Derivative with Deep HOMO level and its application in high-performance polymer solar cells. Angewandte Chemie, 122(8), pp.1542-1545.

[22] Vandewal, K., Tvingstedt, K., Gadisa, A., Inganäs, O. and Manca, J. V., 2009. On the origin of the open-circuit voltage of polymer-fullerene solar cells. Nature Materials, 8 (11), 904–909.

[23] Gadisa, A., Svensson, M., Andersson, M.R. and Inganäs, O., 2004. Correlation between oxidation potential and open-circuit voltage of composite solar cells based on blends of polythiophenes/fullerene derivative. Applied Physics Letters, 84(9), pp.1609-1611.
[24] Brabec, C.J., Cravino, A., Meissner, D., Sariciftci, N.S., Fromherz, T., Rispens, M.T., Sanchez, L. and Hummelen, J.C., 2001. Origin of the open circuit voltage of plastic solar cells. Advanced Functional Materials, 11(5), pp.374-380.
[25] Kumar, K., Das, A., Kumawat, U.K. and Dhawan, A., 2019. Tandem organic solar cells containing plasmonic nanospheres and nanostars for enhancement in short circuit current density. Optics express, 27(22), pp.31599-31620.
[26] Chen, H.Y., Hou, J., Zhang, S., Liang, Y., Yang, G., Yang, Y., Yu, L., Wu, Y. and Li, G., 2009. Polymer solar cells with enhanced open-circuit voltage and efficiency. Nature photonics, 3(11), pp.649-653.
[27] Allen, F.H., Kennard, O., Watson, D.G., Brammer, L., Orpen, A.G. and Taylor, R., 1987. Tables of Bond Lengths determined by X-Ray and Neutron Diffraction. Part I. Bond Lengths in Organic Compounds Journal of the Chemical Society. Perkin Trans, 111987.
[28] Ramos-Cordoba, E., Lambrecht, D.S. and Head-Gordon, M., 2011. Charge-transfer and the hydrogen bond: Spectroscopic and structural implications from electronic structure calculations. Faraday discussions, 150, pp.345-362.

APPENDIX

GRAPHICAL ABSTRACT

Density Functional Theory) DFT Simulations on Fullerene/Polymer blends for Organic Photovoltaic Systems

Rina Muhammad Faisal, Rohini M. de Silva, K.M. Nalin de Silva,

Organic photovoltaics (OPV) has drawn a lot of attention in the world of renewable energy in recent times due to low cost, convenient fabrication processes and high portability. The commercially viable OPV cells possess a power conversion efficiency of only 5-9% even though many researches are underway. This article explores the influence of free energies, interaction energies, relative stability, stability of bonds and charge transfer of computationally designed OPV systems based on Density Functional Theory.

GRAPHICAL ABSTRACT FIGURE